

The Far Ultraviolet Spectral Signatures of Formaldehyde and Carbon Dioxide in Comets

Paul D. Feldman, Roxana E. Lupu, and Stephan R. McCandliss

*Department of Physics and Astronomy, The Johns Hopkins University
3400 N. Charles Street, Baltimore, Maryland 21218*

pdf@pha.jhu.edu

and

Harold A. Weaver

Space Department, Johns Hopkins University Applied Physics Laboratory, 11100 Johns Hopkins Road, Laurel, MD 20723-6099

ABSTRACT

Observations of four comets made with the *Far Ultraviolet Spectroscopic Explorer* show the rotational envelope of the (0,0) band of the CO Hopfield-Birge system ($C^1\Sigma^+ - X^1\Sigma^+$) at 1088 Å to consist of both “cold” and “hot” components, the “cold” component accounting for $\sim 75\%$ of the flux and with a rotational temperature in the range 55–75 K. We identify the “hot” component as coming from the dissociation of CO₂ into rotationally “hot” CO, with electron impact dissociation probably dominant over photodissociation near the nucleus. An additional weak, broad satellite band is seen centered near the position of the P(40) line that we attribute to CO fluorescence from a non-thermal high J rotational population produced by photodissociation of formaldehyde into CO and H₂. This process also leaves the H₂ preferentially populated in excited vibrational levels which are identified by fluorescent H₂ lines in the spectrum excited by solar O VI $\lambda 1031.9$ and solar Lyman- α . The amount of H₂ produced by H₂CO dissociation is comparable to the amount produced by photodissociation of H₂O. Electron impact excitation of CO, rather than resonance fluorescence, appears to be the primary source of the observed $B^1\Sigma^+ - X^1\Sigma^+(0,0)$ band at 1151 Å.

Subject headings: comets: individual (C1999 T1, C/2001 A2, C/2000 WM1, C/2001 Q4) — ultraviolet: solar system

1. INTRODUCTION

In previous papers (Feldman et al. 2002; Weaver et al. 2002; Feldman 2005), we reported on the spectra of four comets observed by the *Far Ultraviolet Spectroscopic Explorer (FUSE)*. Launched in June 1999, *FUSE* operated through October 2007 providing an orbiting capability with a spectral resolution better than 0.4 Å in the wavelength range 905–1187 Å together with very high sensitivity to weak emissions making possible both the search for minor coma species and extensive temperature and density diagnostics for the dominant species. Our initial reports on the three comets observed in 2001 focused on three Hopfield-Birge band systems of CO not previously observed in comets, the $B^1\Sigma^+ - X^1\Sigma^+(0,0)$ band at 1150.5 Å, the $C^1\Sigma^+ - X^1\Sigma^+(0,0)$ band at 1087.9 Å, and the weak $E^1\Pi - X^1\Sigma^+(0,0)$ band at 1076.1 Å, three lines of H₂ fluorescently pumped by solar Lyman- β radiation, and upper limits to emission from O VI and Ar I. The rotational envelopes of the CO bands are resolved and appear to consist of both cold and warm components, the cold component, with a rotational temperature in the range 55–75 K, accounting for over 75% of the flux and presumably due to native CO released by the nucleus. The warm (~500 K) component suggested a CO₂ photodissociation source but this was considered unlikely because the low rate for this process in the solar radiation field would have required a very high relative abundance of CO₂.

O VI emission at 1031.9 and 1037.6 Å was searched for but only the 1031.9 Å line was marginally detected in C/2000 WM1 at about the level predicted by a model used to explain the X-ray emission from comets as being produced by charge exchange between solar wind ions and cometary neutrals (Kharchenko & Dalgarno 2001). The higher signal/noise ratio in the spectrum of comet C/2001 Q4, observed in April 2004, enabled an accurate determination of the wavelength of this feature which suggested that it was the H₂ (1,1) Q(3) Werner ($C^1\Pi_u - X^1\Sigma_g^+$) line, which can be fluorescently pumped by either solar N III λ 989.8 or O VI λ 1031.9. The latter requires the H₂ to be in the first vibrationally excited state (Liu & Dalgarno 1996). The Q(3) lines of the (1,3) band at 1119.1 Å and the (1,4) band at 1163.8 Å are also detected as would be expected for fluorescent excitation. However, the ground state H₂ abundance in the coma, estimated from the solar Lyman- β pumped fluorescence of the Lyman ($B^1\Sigma_u^+ - X^1\Sigma_g^+$) (6,1) P1 line, is insufficient for excitation by solar N III (a factor of 10 weaker than O VI), which implies the formation of H₂ in the $v = 1$ state and excitation by solar O VI.

The molecular channel of the photodissociation of formaldehyde (i.e., the channel leading to H₂ and CO products) has been well studied both experimentally and theoretically. Its products are characterized by a non-thermal rotationally “hot” CO molecule and a vibrationally excited H₂ molecule (van Zee et al. 1993). The CO rotational distribution can be

represented by a gaussian centered near $J = 40$ with a half-width at half maximum in J of about 20. Fluorescence from such levels in the P-branch (the R-branch is shortward of the detector wavelength cut-off) is clearly seen in two of the comets observed by *FUSE* and we propose that this feature, together with the vibrationally excited H_2 , constitute an unambiguous signature of H_2CO in a cometary coma. Formaldehyde has been observed in these comets in both the infrared and millimeter spectral regions (Biver et al. 2006; Milam et al. 2006; Gibb et al. 2007). The capability of *FUSE* to identify H_2CO in a cometary coma provides a new means to determine its production rate relative to that of water and to compare these results with ground-based observations in the infrared and millimeter regions of the spectrum.

Since the thermal “hot” component of the observed CO emission is not produced by H_2CO dissociation, we return to CO_2 as a possible parent, particularly as the rotational temperature is what would be expected based solely on angular momentum conservation arguments (Mumma et al. 1975). We suggest that within the *FUSE* field-of-view, photoelectron impact dissociation of CO_2 has a comparable rate to photodissociation and we base this conclusion on estimates of the mean photoelectron flux derived from the other prominent CO band observed in these spectra, the $B - X$ (0,0) band at 1151 Å. We thus have unique diagnostics in which the shapes of these molecular bands can be used to infer the column abundance of CO from both its native source as well as from two of its direct molecular parents, together with the photoelectron contributions to excitation and dissociation in the inner coma.

2. OBSERVATIONS

Three long period comets were observed during 2001, C/1999 T1 (McNaught-Hartley), C/2001 A2 (LINEAR), and C/2000 WM1 (LINEAR), with C/2001 A2 being the most active of the three and showing the brightest far-ultraviolet emissions. In December 2001, two of the reaction wheels on the spacecraft failed resulting in a shutdown of observatory operations until a new pointing control program could be devised and implemented a few months later. However, no moving target observations were attempted until early in 2004 when comet C/2001 Q4 (NEAT) was observed. The observation parameters for all four comets are summarized in Table 1.

Observations of each comet were made over contiguous spacecraft orbits during which the center of the $30'' \times 30''$ spectrograph aperture was placed at the ephemeris position of the comet and tracked at the predicted sky rate. Due to the extended, though not uniform, nature of the cometary emissions within the aperture, the effective spectral resolution is

~ 0.25 Å. For each comet, all of the orbits of data were co-added and the extracted fluxes were converted to average brightness (in rayleighs) in the $30'' \times 30''$ aperture. In addition, the data were separately co-added for only the time during which the spacecraft was in Earth shadow. These “night-only” spectra make it possible to differentiate cometary emissions of H I, O I, N I, and, in second order, He I, from the same emissions produced in the daytime terrestrial atmosphere (Feldman et al. 2001). For the CO and H₂ emissions this is not a problem and the entire data set for each comet was used.

All of the data were reprocessed using the final version of the *FUSE* pipeline, *Cal-FUSE 3.2* (Dixon et al. 2007). Among the enhancements incorporated in this version were temperature-dependent wavelength corrections, time-dependent corrections to the detector effective areas, and a more complete evaluation of detector background. The latter was particularly significant in allowing reliable extractions of the fluxes of weak emission features. The overall absolute flux calibration, based on standard stars and adjusted for the date of observation, is better than 5%. Table 1 also lists the extracted brightnesses of the CO emission features discussed below.

3. SPECTRA

3.1. Data

The CO $C - X$ (0,0) band, from the total exposure, is shown for each comet in Figure 1. The P and R branches appear well separated, characteristic of a rotational temperature of 55–75 K. There also appear broad wings to the band indicative of a rotational temperature in the range of 500 to 600 K. The figures also show a model fit, assuming solar resonance fluorescence, obtained using the procedure described by Feldman et al. (2002). The derived column densities and rotational temperatures are given in Table 2. In the two most active comets, C/2001 A2 and C/2001 Q4, there is also an additional broad feature centered at ~ 1089.4 Å, that we identify as P-branch lines from high-lying J states. The position of the P(40) line, calculated using the rotational constants of Eidelsberg et al. (1991), is also shown in Fig. 1. We note that the Eidelsberg et al. wavelengths have been verified experimentally only up to $J = 25$. The corresponding high J R-lines are off the short wavelength edge of the LiF2a detector. A “hot” thermal rotational distribution arises in molecular photodissociation in order to conserve angular momentum when the product molecule has a much smaller moment-of-inertia than the parent molecule as is the case for CO₂ (Mumma et al. 1975). The non-thermal component is identified with CO as a dissociation product of H₂CO, and the column abundance of this component, also given in Table 2, is derived assuming an equal contribution from the unobserved R-branch. In this case, an optically thin band

fluorescence efficiency is used as the CO population is spread over many rotational levels and the absorption is not likely to be optically thick.

3.2. Photodissociation of Formaldehyde

As noted above, the photodissociation of formaldehyde has been intensively studied, both experimentally and theoretically. The lowest dissociation threshold ($\sim 3600 \text{ \AA}$) leads to $\text{H}_2 + \text{CO}$ (the “molecular” channel) while $\sim 2700 \text{ cm}^{-1}$ higher ($\sim 3300 \text{ \AA}$), $\text{H} + \text{HCO}$ (the “radical” channel) can also be produced (van Zee et al. 1993). The nature of the H_2 and CO products differs markedly above and below this second energy threshold. Consider first the region below the radical channel threshold. Bamford et al. (1985) and Debarre et al. (1985) have used laser-induced fluorescence spectroscopy and coherent anti-Stokes Raman scattering to experimentally study the product state populations of CO and H_2 . Bamford et al. found a nonthermal highly excited CO rotational population with a Gaussian distribution centered at $J = 40$ and a half-width at half maximum of 20 J units, but with little vibrational excitation. Later work (e.g., van Zee et al. 1993) showed that the shape was dependent on the energy of the absorbed photon. It should be noted that the absorption of H_2CO in this region is in discrete bands (Rogers 1990). For H_2 , Debarre et al. found that the primary products are the ortho ($J = 3$ and 5) states of $v = 1$. For photolysis at 3390 \AA they found the fractional population of the $v = 1$, $J = 3$ level to be 11%. Butenhoff et al. (1990) extended this work to additional wavelengths and found a peak H_2 population in $v = 1$, $J = 3$.

Above the radical channel threshold, H_2 and CO are found to have markedly different populations with the non-translational energy going principally to vibrational excitation of H_2 while the CO rotational state population shifts to lower J states (van Zee et al. 1993). Zhang et al. (2005) demonstrated that the population of vibrationally excited H_2 , up to $v = 8$ or 9, increased as the energy of the exciting photon increased with a corresponding increase in the low- J state population of CO such that the non-translational energy was conserved. However, the peak at $J = 40$ remained and the low- J population was still highly non-thermal. Chambreau et al. (2006) showed that the excited vibrational levels of H_2 also had peak rotational populations at $J = 5$ or 7, depending on the photolysis energy.

In the solar radiation field in the coma of a comet, the H_2 and CO state populations derived from H_2CO dissociation will reflect a superposition of populations, weighted by the solar flux and absorption cross section (Huebner et al. 1992). Such a calculation is beyond the scope of the present paper. The broad, weak feature seen longward of the $C - X$ (0,0) band in comets C/2001 A2 and C/2001 Q4 in Fig. 1 is centered near the position of the P(40) line of this band, and the non-thermal high- J population of this feature is

an unambiguous fingerprint of CO produced from H₂CO photodissociation. Although the spectrum of C/2000 WM1 is significantly noisier, the data also suggest enhanced emission on the red wing of the band in this comet. Further evidence for this source is the simultaneous detection of fluorescence from vibrationally excited H₂ in this comet (Liu et al. 2007) as well as in comets C/2001 A2 and C/2001 Q4.

3.3. Fluorescence of Vibrationally Excited H₂

In Figure 2 the region of the O VI doublet in comet C/2001 Q4 is shown, and the H₂ (1,1) Q(3) line is identified, separated by 0.06 Å from the position of the O VI line at 1031.92 Å. The uncertainty in the *FUSE* wavelength scale is ~ 0.01 Å. The same figure also shows the corresponding (1,3) Q(3) and (1,4) Q(3) lines at 1119.09 and 1163.79 Å, respectively (Liu & Dalgarno 1996). Note that there is no emission at the expected position of the O VI line at 1037.62 Å. These lines are quite weak and with the exception of a 3- σ detection in comet C/2000 WM1 (Liu et al. 2007) do not appear in the spectra of the two other comets observed by *FUSE*.

The absence of these lines in the other two comets is the result of the heliocentric Doppler shift of the exciting solar line, the Swings effect (Feldman et al. 2004), rather than the lack of H₂ in the coma. This can be illustrated with the solar O VI $\lambda 1031.9$ line profile. Doschek & Feldman (2004) have used the recent solar spectra taken by the SUMER instrument on *SOHO* with an instrumental resolution of ~ 0.1 Å, to determine the width of this line under quiet sun conditions to be 0.202 Å. This result is from an observation of a small part of the solar disk near the center, while for the calculation of cometary excitation rates the whole disk flux is more useful. Fortunately, we are able to take advantage of a minor operational problem of *FUSE* (Sahnou et al. 2000), a sensitivity at certain orientations on the sky of the silicon carbide (SiC) channels to scattered solar radiation, to determine the whole disk line shape. The observation of comet C/2001 Q4 resulted in such an orientation and the SiC1b and SiC1a channels (905–992 and 1005–1090 Å, respectively) measured a large scattered solar flux in all three apertures. Both the high (HIRS, $1''.5 \times 20''$) and medium resolution (MDRS, $4'' \times 20''$) apertures obtained good S/N spectra of the O VI lines at instrumental resolutions of 0.035 and 0.075 Å, respectively. From both of these channels we derived a width of 0.200 Å for the solar O VI $\lambda 1031.9$ line, in excellent agreement with the result of Doschek & Feldman. The MDRS profile is shown in Figure 3, together with the Doppler shifted positions of the H₂ (1,1) Q(3) line for each comet. Note that the profile shown in the figure suggests that the solar line is not adequately represented by a single Gaussian. Clearly, the detection of the (1, v'') lines in comet C/2001 Q4 was favored by its

negative heliocentric velocity and by the relatively high activity level of this comet at the time of observation.

Wolven et al. (1997) noted that solar Lyman- α (1216.57 Å) could pump vibrationally excited H₂ in the $v = 2$ level via the Lyman band (1,2) P(5) and R(6) lines, and used this mechanism to identify fluorescence from the upper level in *Hubble Space Telescope* spectra of Jupiter following the impact of comet Shoemaker-Levy 9 in July 1994. The same mechanism has recently been found to operate in planetary nebulae where the *FUSE* spectra show the (1,1) P(5) and R(6) lines at 1161.82 and 1161.95 Å, respectively (Lupu et al. 2006). One of the previously unidentified lines reported in *FUSE* spectra of comets at 1161.83 Å was identified by Liu et al. (2007) as a blend of these two H₂ lines (see Fig. 2). The vibrationally excited H₂ would most likely come from H₂CO rather than H₂O photodissociation as proposed by Liu et al. This feature has roughly the same brightness in comets C/2001 A2 and C/2001 Q4, and we note that the brightnesses of the CO P(40) feature in these two comets are also comparable. From the branching ratios given by Lupu et al., we would also expect to see the (1,1) R(3) line at 1148.70 Å and the (1,1) P(8) line at 1183.31 Å from the same excited J levels, and indeed we do. The latter is considerably weaker than the former due to the lower population of the even- J (para) states as expected.

Liu et al. also identified several other cometary lines as being pumped by solar Lyman- α from higher vibrational and rotational levels of H₂. Almost all of the strong unidentified features tabulated by Feldman (2005) are amongst them. Our analysis supports the conclusion of Liu et al. that the vast majority of emission features in the *FUSE* spectra of comets can be attributed to H₂. However, unlike Liu et al., who proposed that the excited vibrational and rotational levels of H₂ arise from the photodissociation of H₂O, we suggest instead that these excited H₂ states are produced during the photodissociation of H₂CO because their presence in the cometary coma is consistent with the H₂ level populations measured during H₂CO photodissociation in the laboratory by Zhang et al. (2005) and Chambreau et al. (2006).

3.4. Electron Impact Excitation of CO and Dissociation of CO₂

The CO $B - X$ (0,0) band at 1151 Å is weaker than the $C - X$ (0,0) band by a factor of 3 to 4 and thus recorded with poorer signal/noise in all four comets as shown in Figure 4. It is surprising that this band is observed at all since its fluorescence efficiency is 44 times lower than that of the $C - X$ (0,0) band (the predicted spectra using the CO column densities given in Table 2 are also shown in the figure). There must be an additional source of excitation, and since the band shape is consistent with the low temperature CO component, that can only be electron impact excitation of CO. Photoelectrons in the inner comae of comets have

been considered by several authors (e.g., Ashihara 1978; Körösmezey et al. 1987), and were detected in the *Vega* fly-by of 1P/Halley (Gringauz et al. 1986), but their role in excitation, dissociation and ionization is difficult to quantify.

An equivalent to the fluorescence efficiency, or g-factor, may be defined by an electron excitation rate per molecule per second, g' :

$$g' = \int \int F(E)\sigma(E)dEd\Omega$$

where $F(E)$ is the photoelectron flux in electrons $\text{s}^{-1}\text{cm}^{-2}\text{sr}^{-1}\text{eV}^{-1}$ and $\sigma(E)$ is the cross section in cm^2 . In general, the photoelectron flux is a function of cometocentric distance and is anisotropic so that g' will vary over the spectrograph field-of-view.

Rather than attempt to use modeled photoelectron fluxes, we instead use the observed CO $B - X$ (0,0) band brightnesses to derive an effective g' over the *FUSE* aperture but then use the modeled electron energy distribution to determine the relative excitation rates for other processes. In particular, we are interested in the electron impact dissociation rate of CO_2 . Relevant cross sections in analytic form for electron impact on CO and CO_2 are available from the compilation of Shirai et al. (2001). Figure 5 shows the cross sections for electron impact excitation on CO of the two bands under discussion and that for electron impact dissociation of CO_2 into the metastable $a^3\Pi$ state of CO. A typical photoelectron energy dependence, from Körösmezey et al. (1987), is also shown. The $a^3\Pi$ state is the upper level of the CO Cameron bands, whose excitation in comets has been discussed by Weaver et al. (1994). The total CO_2 dissociation cross section has been studied by Cosby & Helm (1992). These authors note that the branching ratio into the $a^3\Pi$ state of CO is 27% of the total electron dissociation rate, the same as for solar photodissociation (Huebner et al. 1992).

The derived values of g' , reduced to 1 AU, are given in Table 3. For comparison, the optically thin solar fluorescence efficiencies are also given. Figure 5 shows that the steep increase of photoelectron flux towards lower energies favors the $B - X$ transitions over the $C - X$. Even so, the electron impact contribution to C state excitation will reduce the derived CO column abundances by 5–15% and this is reflected in the values given in Table 2. These numbers remain uncertain as both the photoelectron energy distribution and flux will vary with increasing column density towards the nucleus. This will also affect the ratio of total CO_2 dissociation to that fraction leading to the $a^3\Pi$ state of CO. The g' values for these processes, for the photoelectron model adopted, are also given in Table 3. For comparison with photodissociation at 1 AU, the solar maximum value given by Huebner et al. (1992) is $2.56 \times 10^{-6} \text{ molecule}^{-1} \text{ s}^{-1}$, so electron impact dissociation and photodissociation are comparable.

Evidence for a significant role of photoelectrons in the inner coma has often been noted in the literature. Two particular cases in which photodissociation and photoionization were inadequate to account for the abundance of daughter products are the production of atomic carbon in the metastable ^1D state from CO (Tozzi et al. 1998) and the high concentration of CO_2^+ close to the nucleus seen in early *IUE* spectra (Festou et al. 1982). The *FUSE* spectra provide additional evidence in the strong O I $^1\text{D} - ^1\text{D}^o$ line at 1152.16 Å, seen in Fig. 4, which also cannot be accounted for by solar resonance scattering alone. The lower state of this transition, the metastable ^1D state, is an abundant product of photodissociation of H_2O , OH, and CO, and is the upper level of the oxygen “red” lines at 6300 and 6364 Å, seen in many comets and often used as a surrogate for the water production rate (Feldman et al. 2004).

4. DISCUSSION

4.1. Modeling

The column density of the non-thermal component of CO was modeled assuming an H_2CO parent using the vectorial model of Festou (1981) with solar photodestruction rates given by Huebner et al. (1992). Meier et al. (1993) have also evaluated the photodissociation lifetimes (H_2CO has two other dissociation channels, $\text{H} + \text{HCO}$, and $\text{H} + \text{H} + \text{CO}$) and find the rate into $\text{H}_2 + \text{CO}$ to be 25% lower than that of Huebner et al. while the total rate is 7% lower. Bockelée-Morvan & Crovisier (1992) find a total photodissociation lifetime in close agreement with that of Huebner et al. The model assumes a nucleus source for the H_2CO . Even if a distributed source were present (see Section 4.4 below), the size of the *FUSE* aperture translates to a few thousand km projected on the sky and such a source can be ignored for our purposes.

To determine production rates relative to water, we use values of $Q_{\text{H}_2\text{O}}$ taken from the recent literature; values derived from SOHO/SWAN measurements of cometary Lyman- α emission by Combi et al. (2008), and those derived from ODIN submillimeter observations of H_2O directly by Biver et al. (2007). Where they overlap, these two sets of values are in agreement to $\sim 20\text{--}25\%$. We adopt the values from Combi et al. because of their finer sampling grid, allowing us to use data from the same day as the *FUSE* observations. We use the deconvolved model results from Combi et al. rather than the daily averages given. For C/2001 Q4 we use a value derived from near-simultaneous *HST* observations of OH emission, which is close to that reported by Biver et al.

For C/2001 A2 we note a significant difference from the value of $Q_{\text{H}_2\text{O}}$ cited in the initial

reports of the *FUSE* observations by Feldman et al. (2002) and Weaver et al. (2002). The earlier estimate was based on a visual outburst two days prior to the observation and a modeled production rate adjusted to match the derived H_2 column density. The latter was based on fluorescence efficiencies derived by Krasnopolsky & Feldman (2001). With the availability of detailed solar Lyman- β fluxes and line shapes from SOHO/SUMER (Lemaire et al. 2002), the heliocentric velocity dependent g-factors were recalculated and the H_2 column density revised downward by a factor of about three, which is consistent with the water production rate for the date given by Combi et al.

The results are given in Table 4. For the comets in which the non-thermal CO is detected, the production rates of H_2CO relative to that for H_2O are generally in the range of values found from infrared and millimeter observations. Biver et al. (2006) reported on four comets observed at millimeter wavelengths including the three comets observed by *FUSE* at comparable epochs in 2001. For comets C/2001 A2 and C/2000 WM1, our relative production rates are comparable to those of Biver et al. based on their model that assumes a distributed source with an effective parent lifetime about a factor of 2 longer than the true photochemical lifetime. With an assumed H_2CO parent, Biver et al. derive relative production rates 2 – 4 times smaller.

Millimeter observations of comet C/2001 Q4 were made in mid-May 2004 by Milam et al. (2006). Their results for H_2CO , again assuming a distributed grain source, are in close agreement with the *FUSE* value. While infrared bands of H_2CO near $3.6 \mu\text{m}$ have been detected in a number of recent comets, the only data available for comparison with the *FUSE* observations is of C/2001 A2 (Gibb et al. 2007). Gibb et al., observing 2 and 3 days prior to the *FUSE* observation, found a low value of 0.24% for the ratio of the production rate of H_2CO relative to H_2O on July 9.5 followed by a decrease of a factor of 4 one day later. In contrast, we derive a much higher value for this ratio on July 12.5. The apparent variability of H_2CO is discussed below in Section 4.2.

Modeling the H_2 brightness is not as straightforward. The H_2 molecules initially carry away most of the excess energy of dissociation as translational energy ($\sim 11 \text{ km s}^{-1}$), but they are rapidly thermalized in the inner coma (Combi et al. 2004). The excited state populations will also vary with incident wavelength and be altered by collisions, so the actual number of H_2 molecules in the $v = 1, J = 3$ level produced by solar photodissociation will have a large uncertainty. Nevertheless, as a consistency check we can evaluate the number of such molecules in the field-of-view needed to produce the observed 0.13 rayleigh brightness of the (1,1) Q(3) line at 1031.86 \AA observed in comet C/2001 Q4. The fluorescence efficiency, or g-factor, at the peak of the solar O VI line is calculated using the solar minimum irradiance recommended by Warren (2005) and the oscillator strengths and branching ratios taken from

the compilation of Abgrall et al. (1993b). The derived g-factor is $3.8 \times 10^{-7} \text{ s}^{-1} \text{ molecule}^{-1}$ at 1 AU, so that a mean column density of $3.6 \times 10^{11} \text{ cm}^{-2}$ is sufficient to produce the observed emission rate. From Table 2, the column density of non-thermal CO in this comet is $4.1 \times 10^{12} \text{ cm}^{-2}$, and 78% of those are accompanied by H₂ rather than by two H atoms (Huebner et al. 1992). Thus 11% of the total H₂ needs to be in $v = 1, J = 3$, which is plausible based on the laboratory data of Zhang et al. (2005) and Chambreau et al. (2006). Given all of the uncertainties, this is good agreement and supports our proposal that H₂CO is the source of both the non-thermal CO and the vibrationally excited H₂ detected by *FUSE*.

The H₂ vibrational population may also be examined with the identification of solar Lyman- α pumping of lines in the Lyman (1,2) band as described in Section 3.3. The solar Lyman- α spectral flux is roughly two orders of magnitude larger than that of O VI $\lambda 1031.9$ resulting in comparably larger fluorescence efficiencies for these lines. Using solar minimum Lyman- α fluxes from Lemaire et al. (2002) and molecular data for the Lyman bands from Abgrall et al. (1993a), the g-factors for the (1,1) P(5) and R(6) lines can be calculated. The relative population of the $v = 2, J = 5$, needed to account for the observed 1161.8 Å emission of 0.24 rayleighs is 2%. This is consistent with the relative population of this level seen in the laboratory experiments (Zhang et al. 2005), when we consider that these experiments are done at discrete wavelengths while in the cometary context photodissociation is produced by the wavelength integrated solar flux.

We conclude that photodissociation of H₂CO is sufficient to produce vibrationally excited H₂ that accounts for the presence of Lyman- α excited fluorescence of H₂ in the coma. While the production rate of H₂CO is $\sim 0.5\%$ relative to H₂O, the solar photodissociation rate into H₂ is ~ 100 times higher for H₂CO, depending on the solar activity level (Huebner et al. 1992). Thus both molecules contribute comparable amounts of H₂ to the coma. The branching of water photodissociation into H₂ + O(¹D) has also been studied in the laboratory (Slanger & Black 1982), but there are no available measurements of the resultant H₂ level populations. Although there has been extensive theoretical work on the H + OH channel of H₂O photodissociation (Schinke 1993), there does not seem any devoted to the H₂ + O(¹D) channel, which is clearly warranted. On the basis of the brightness of the Lyman- β pumped fluorescent lines, Feldman et al. (2002) suggested that solar photodissociation of water led to a thermal population of H₂ molecules in the $v = 0, J = 1$ level.

4.2. Caveat on Temporal Variability

We noted above the utility of the SOHO/SWAN data of Combi et al. (2008) to obtain daily values of the water production rate. For C/2001 A2 near the time of the *FUSE* ob-

servations, the comet exhibited several visual outbursts, particularly one on 2001 July 11.5, one day before the *FUSE* observations, which saw a 1.5 magnitude increase in visual brightness (Sekanina et al. 2002). These outbursts were reflected in sudden increases in $Q_{\text{H}_2\text{O}}$ of factors of 2–3 in one day in the data of Combi et al.. The *FUSE* observations of this comet spanned 7.5 hours during which the CO emission decreased by a factor of two (Fig. 6), likely a manifestation of the decrease in coma abundance following the outburst. Note that for this comet the *FUSE* $30'' \times 30''$ aperture projects to 6500×6500 km on the sky so that a molecule moving radially outward at 1 km s^{-1} would exit the field-of-view in less than one hour. Hence the observed variation represents variability of the CO source on this time scale. On the other hand, the column densities given in Table 2 are taken from the summed spectra (to improve the signal/noise ratio) and thus represent average values. Caution is therefore urged in deriving relative production rates from diverse observations, even if obtained on the same date, and in the comparison of results from different observers.

The July 11.5 outburst makes it difficult to compare the derived H_2CO production rates of Gibb et al. (2007) on July 9.5 and 10.5, noted above, with the present results. From the limited data available, it is not possible to determine whether H_2CO production was enhanced by the outburst or whether the increase inferred from the *FUSE* spectra is just the result of intrinsic variability responsible for the change seen by Gibb et al. a few days earlier. The same holds for a comparison of our results with the CO production rate derived from the same infrared spectrum on July 10.5 (Magee-Sauer et al. 2008) even though in this case the values of Q_{CO} are comparable.

A similar caveat applies to comet C/2001 Q4 which *FUSE* observed over a 27 h period. The variation of the CO emission is shown in Fig. 7 and can be fit with a sinusoidal curve of period 17.0 h and 22% amplitude. Yet the CO production rate, derived from *HST*/STIS observations of the CO Fourth Positive system (Lupu et al. 2007), made near a minimum in the *FUSE* lightcurve, is consistent with the mean value derived from the *FUSE* spectra. In contrast, comet C/2001 WM1 showed little variation in CO emission over a 60 h period. For this comet, simultaneous *HST*/STIS observations were also obtained and Lupu et al. derived comparable CO production rates from both sets of spectra.

4.3. Relative Abundance of CO_2

As noted in Section 3.4, for molecules with long lifetimes against solar photodissociation such as CO_2 , electron impact dissociation becomes an important destruction channel. Using the electron impact rates given in Table 3, however, would still require an abnormally large ($\geq 20\%$) abundance of CO_2 to account for the derived “hot” CO column density. Since

there are no other suitable parents for CO other than CO₂ and H₂CO, it is likely that the model used to calculate the values given in Table 3 significantly underestimates the electron impact contribution to CO₂ dissociation. Cosby & Helm (1992) note that the threshold for this process is at 7.4 eV whereas the channel leading to the $a^3\Pi$ state of CO requires 11.4 eV. At low electron energies, the model of Körösmezey et al. (1987) does not match the data of Gringauz et al. (1986), which appears to follow an E^{-1} distribution, so that there may be an additional large contribution to the dissociation rate from low energy electrons. There are also uncertainties in the radial and angular distribution of the electrons that make our estimate quantitatively unreliable. A more complete analysis of cometary photoelectrons, which is beyond the scope of the present paper, would entail an analysis of CO Cameron band emission similar to that presented by Weaver et al. (1994). Fortunately, relevant *HST*/STIS spectra do exist for comet C/2001 Q4 and will be treated in a separate publication.

4.4. Distributed Source of CO

The first evidence for a distributed source of CO in the coma of a comet came from the *in situ* Neutral Mass Spectrometer experiment on the *Giotto* mission to comet 1P/Halley (Eberhardt et al. 1987; Eberhardt 1999). Meier et al. (1993) also showed, from the same data set, that the H₂CO also appeared to come from an extended source and that the H₂CO was sufficient to account for the extended CO (Eberhardt 1999). Polyoxymethylene (POM), evaporated from organic material on refractory grains, has been postulated as the source of this H₂CO (Cottin et al. 2004). In recent years, as high resolution spectroscopic instrumentation in the near infrared has made the observation of CO in comets almost routine, considerable effort has been expended in trying to determine if such distributed sources are common or unique to certain comets (Bockelée-Morvan et al. 2004). Identification of a distributed emission source is based on long-slit spectroscopy in which the spatial profile of the emission deviates from that expected for radial outflow (DiSanti et al. 2001; Brooke et al. 2003). For CO this can be done in both the infrared and the ultraviolet.

This approach is applicable only to the brightest comets because the spatial pixels along the slit must be small enough to provide adequate spatial resolution. For such comets, such as C/1995 O1 (Hale-Bopp), the CO column densities along the line-of-sight (to both the Sun and to the observer) are sufficiently large that optical depth effects tend to produce a flattening of the spatial profile near the nucleus that mimics the effect of a distributed source (the ultraviolet case has been discussed by Lupu et al. 2007). This concern was addressed by DiSanti et al. in their analysis of CO in comet Hale-Bopp. They found a very high production rate of CO relative to that of water, 24.1%, with half being from the nucleus and

the other half from a distributed source. In the same comet, Brooke et al. (2003) found an even higher relative abundance of CO, 37–41%, with 90% coming from a distributed source. Bockelée-Morvan et al. (2005) questioned both of these results suggesting that they were the effect of a large infrared opacity, even though both DiSanti et al. and Brooke et al. accounted for opacity effects. In any case, if such a distributed source were H₂CO it would imply an abundance in this comet an order of magnitude higher than that cited by Biver et al. (2006).

5. CONCLUSION

Spectroscopic observations of four comets by *FUSE* have opened a new window for the investigation of the physics and chemistry of the cometary coma. The high spectral resolution of *FUSE* has made it possible to separate the multiple components of the CO emission, while the high sensitivity has allowed the detection of fluorescent H₂ emission pumped by solar O VI radiation. Both of these can be understood in terms of the dissociation processes of H₂CO and CO₂. Despite the small sample, it is clear that previous ultraviolet spectroscopic observations of CO in comets including those from sounding rockets, *IUE* and *HST* (e.g., Feldman et al. 1997) probably included these additional components of CO that were not resolved, either spectrally or spatially, from the native (“cold”) CO with the instrumentation used. Photoelectron excitation contributes ~10% of the observed emission of the CO *C – X* (0,0) band and needs to be accounted for in deriving CO production rates from *FUSE* observations.

We thank the *FUSE* ground system personnel, particularly B. Roberts, T. Ake, A. Berman, B. Gawne, and J. Andersen, for their efforts in planning and executing these moving target observations. This work is partially based on data obtained for the Guaranteed Time Team by the NASA-CNES-CSA *FUSE* mission operated by the Johns Hopkins University. Financial support was provided by NASA contract NAS5-32985 and NASA grant NAG5-12963.

Facilities: FUSE ()

REFERENCES

- Abgrall, H., Roueff, E., Launay, F., Roncin, J. Y., & Subtil, J. L. 1993a, *A&AS*, 101, 273
- Abgrall, H., Roueff, E., Launay, F., Roncin, J. Y., & Subtil, J. L. 1993b, *A&AS*, 101, 323
- Ashihara, O. 1978, *Icarus*, 35, 369
- Bamford, D. J., Filseth, S. V., Foltz, M. F., Hepburn, J. W., & Moore, C. B. 1985, *J. Chem. Phys.*, 82, 3032
- Biver, N., et al. 2007, *Planet. Space Sci.*, 55, 1058
- Biver, N., et al. 2006, *A&A*, 449, 1255
- Bockelée-Morvan, D., Boissier, J., Crovisier, J., Henry, F., & Weaver, H. A. 2005, *BAAS*, 37, 633
- Bockelée-Morvan, D., & Crovisier, J. 1992, *A&A*, 264, 282
- Bockelée-Morvan, D., Crovisier, J., Mumma, M. J., & Weaver, H. A. 2004, in *Comets II*, ed. M. C. Festou, H. A. Weaver, & H. U. Keller (Tucson: Univ. of Arizona), 391
- Brooke, T. Y., Weaver, H. A., Chin, G., Bockelée-Morvan, D., Kim, S. J., & Xu, L.-H. 2003, *Icarus*, 166, 167
- Butenhoff, T. J., Carleton, K. L., & Moore, C. B. 1990, *J. Chem. Phys.*, 92, 377
- Chambreau, S. D., Lahankar, S. A., & Suits, A. G. 2006, *J. Chem. Phys.*, 125, 044302
- Combi, M. R., Harris, W. M., & Smyth, W. H. 2004, in *Comets II*, ed. M. C. Festou, H. A. Weaver, & H. U. Keller (Tucson: Univ. of Arizona), 523
- Combi, M. R., Mäkinen, J. T. T., Henry, N. J., Bertaux, J.-L., & Quemérais, E. 2008, *AJ*, 135, 1533
- Cosby, P. C., & Helm, H. 1992, *Dissociation rates of diatomic molecules*, Technical report, SRI International
- Cottin, H., Bénilan, Y., Gazeau, M.-C., & Raulin, F. 2004, *Icarus*, 167, 397
- Debarre, D., Lefebvre, M., Péalat, M., Taran, J.-P. E., Bamford, D. J., & Moore, C. B. 1985, *J. Chem. Phys.*, 83, 4476
- DiSanti, M. A., Mumma, M. J., Russo, N. D., & Magee-Sauer, K. 2001, *Icarus*, 153, 361

- Dixon, W. V., et al. 2007, *PASP*, 119, 527
- Doschek, G. A., & Feldman, U. 2004, *ApJ*, 600, 1061
- Eberhardt, P. 1999, *Space Science Reviews*, 90, 45
- Eberhardt, P., et al. 1987, *A&A*, 187, 481
- Eidelsberg, M., Benayoun, J. J., Viala, Y., & Rostas, F. 1991, *A&AS*, 90, 231
- Feldman, P. D. 2005, *Physica Scripta*, T119, 7
- Feldman, P. D., Cochran, A. L., & Combi, M. R. 2004, in *Comets II*, ed. M. C. Festou, H. A. Weaver, & H. U. Keller (Tucson: Univ. of Arizona), 425
- Feldman, P. D., Festou, M. C., Tozzi, G. P., & Weaver, H. A. 1997, *ApJ*, 475, 829
- Feldman, P. D., Sahnou, D. J., Kruk, J. W., Murphy, E. M., & Moos, H. W. 2001, *J. Geophys. Res.*, 106, 8119
- Feldman, P. D., Weaver, H. A., & Burgh, E. B. 2002, *ApJ*, 576, L91
- Festou, M. C. 1981, *A&A*, 95, 69
- Festou, M. C., Feldman, P. D., & Weaver, H. A. 1982, *ApJ*, 256, 331
- Gibb, E. L., Disanti, M. A., Magee-Sauer, K., Dello Russo, N., Bonev, B. P., & Mumma, M. J. 2007, *Icarus*, 188, 224
- Gringauz, K. I., et al. 1986, *Nature*, 321, 282
- Huebner, W. F., Keady, J. J., & Lyon, S. P. 1992, *Solar photo rates for planetary atmospheres and atmospheric pollutants* (Dordrecht; Boston: Kluwer Academic)
- Kharchenko, V., & Dalgarno, A. 2001, *ApJ*, 554, L99
- Körösmezey, A., et al. 1987, *J. Geophys. Res.*, 92, 7331
- Krasnopolsky, V. A., & Feldman, P. D. 2001, *Science*, 294, 1914
- Lemaire, P., Emerich, C., Vial, J.-C., Curdt, W., Schühle, U., & Wilhelm, K. 2002, in *From Solar Min to Max: Half a Solar Cycle with SOHO*, ed. A. Wilson (Noordwijk: ESA SP-508), 219
- Liu, W., & Dalgarno, A. 1996, *ApJ*, 462, 502

- Liu, X., Shemansky, D. E., Hallett, J. T., & Weaver, H. A. 2007, *ApJS*, 169, 458
- Lupu, R. E., Feldman, P. D., Weaver, H. A., & Tozzi, G.-P. 2007, *ApJ*, 670, 1473
- Lupu, R. E., France, K., & McCandliss, S. R. 2006, *ApJ*, 644, 981
- Magee-Sauer, K., Mumma, M. J., Disanti, M. A., Dello Russo, N., Gibb, E. L., Bonev, B. P., & Villanueva, G. L. 2008, *Icarus*, 194, 347
- Meier, R., Eberhardt, P., Krankowsky, D., & Hodges, R. R. 1993, *A&A*, 277, 677
- Milam, S. N., et al. 2006, *ApJ*, 649, 1169
- Mumma, M. J., Stone, E. J., & Zipf, E. C. 1975, *J. Geophys. Res.*, 80, 161
- Rogers, J. D. 1990, *J. Phys. Chem.*, 94, 4011
- Sahnou, D. J., et al. 2000, *ApJ*, 538, L7
- Schinke, R. 1993, *Photodissociation Dynamics - Spectroscopy and Fragmentation of Small Polyatomic Molecules* (Cambridge: Cambridge University Press)
- Sekanina, Z., Jehin, E., Boehnhardt, H., Bonfils, X., Schuetz, O., & Thomas, D. 2002, *ApJ*, 572, 679
- Shirai, T., Tabata, T., & Tawara, H. 2001, *Atomic Data and Nuclear Data Tables*, 79, 143
- Slanger, T. G., & Black, G. 1982, *J. Chem. Phys.*, 77, 2432
- Tozzi, G. P., Feldman, P. D., & Festou, M. C. 1998, *A&A*, 330, 753
- van Zee, R. D., Foltz, M. F., & Moore, C. B. 1993, *J. Chem. Phys.*, 99, 1664
- Warren, H. P. 2005, *ApJS*, 157, 147
- Weaver, H. A., Feldman, P. D., Combi, M. R., Krasnopolsky, V., Lisse, C. M., & Shemansky, D. E. 2002, *ApJ*, 576, L95
- Weaver, H. A., Feldman, P. D., McPhate, J. B., A'Hearn, M. F., Arpigny, C., & Smith, T. E. 1994, *ApJ*, 422, 374
- Wolven, B. C., Feldman, P. D., Strobel, D. F., & McGrath, M. A. 1997, *ApJ*, 475, 835
- Zhang, X., Rheinecker, J. L., & Bowman, J. M. 2005, *J. Chem. Phys.*, 122, 4313

Table 1: Comet observation parameters and observed CO brightnesses.

Comet	C/1999 T1 (McNaught-Hartley)	C/2001 A2 (LINEAR)	C/2000 WM1 (LINEAR)	C/2001 Q4 (NEAT)
Date	2001 Feb 3	2001 Jul 12	2001 Dec 7–10	2004 Apr 24
Start Time (UT)	17:43	13:48	08:48	00:40
Exposure Duration (s)	15,614	15,063	36,467	68,282
r (AU)	1.43	1.20	1.12	1.03
Δ (AU)	1.29	0.30	0.34	0.51
\dot{r} (km s ⁻¹)	14.9	22.8	-28.3	-10.8
$F_{10.7}$ (sfu)	160	140	220	115
$C - X$ (0,0) (rayleighs)	1.46 ± 0.03	2.47 ± 0.04	0.74 ± 0.02	6.29 ± 0.03
...P(40) peak (rayleighs)	≤ 0.02	0.16 ± 0.03	0.10 ± 0.01	0.16 ± 0.02
$B - X$ (0,0) (rayleighs)	0.19 ± 0.02	0.71 ± 0.03	0.16 ± 0.01	1.51 ± 0.02

Table 2: Derived CO column densities and rotational temperatures in the *FUSE* 30'' \times 30'' aperture. Errors are from the 1 σ contours in a three parameter fit.

Comet	C/1999 T1 (McNaught-Hartley)	C/2001 A2 (LINEAR)	C/2000 WM1 (LINEAR)	C/2001 Q4 (NEAT)
N_{cold} (cm ⁻²)	$(3.5 \pm 0.2) \times 10^{13}$	$(2.7 \pm 0.15) \times 10^{13}$	$(6.0 \pm 0.4) \times 10^{12}$	$(1.55 \pm 0.05) \times 10^{14}$
N_{hot} (cm ⁻²)	$\leq 1.3 \times 10^{12}$	$(1.10 \pm 0.06) \times 10^{13}$	$(2.5 \pm 0.5) \times 10^{12}$	$(2.0 \pm 0.1) \times 10^{13}$
$N_{\text{non-thermal}}$ (cm ⁻²) ^a	$\leq 0.8 \times 10^{12}$	$(4.5 \pm 0.7) \times 10^{12}$	$(2.5 \pm 0.3) \times 10^{12}$	$(3.3 \pm 0.3) \times 10^{12}$
T_{cold} (K)	59 ± 5	56 ± 7	75 ± 10	58 ± 2
T_{hot} (K)	500	500	500	600

^aAssumes an equal contribution from the R(40) peak not observed. Uncertainties are 1 σ in the counting statistics.

Table 3: Derived effective electron impact excitation rates (g'), in molecule⁻¹ s⁻¹, averaged over the *FUSE* aperture.

Comet	C/1999 T1 (McNaught-Hartley)	C/2001 A2 (LINEAR)	C/2000 WM1 (LINEAR)	C/2001 Q4 (NEAT)
$B - X$ (0,0) ^a	9.0×10^{-9}	2.4×10^{-8}	2.1×10^{-8}	7.4×10^{-9}
$C - X$ (0,0) ^a	5.8×10^{-9}	1.6×10^{-8}	1.3×10^{-8}	4.7×10^{-9}
$a - X$ (all bands) ^b	2.6×10^{-7}	7.1×10^{-7}	6.1×10^{-7}	2.2×10^{-7}
total dissociation ^b	1.1×10^{-6}	2.9×10^{-6}	2.4×10^{-6}	8.6×10^{-7}

^aelectron impact on CO at 1 AU. For comparison, the optically thin fluorescence efficiencies for the $B - X$ (0,0) and $C - X$ (0,0) bands at 1 AU are 2.3×10^{-9} and 1.0×10^{-7} molecule⁻¹ s⁻¹, respectively, for solar maximum conditions.

^belectron impact on CO₂ at 1 AU.

Table 4: Modeled production rates and production rate ratios.

Comet	C/1999 T1 (McNaught-Hartley)	C/2001 A2 (LINEAR)	C/2000 WM1 (LINEAR)	C/2001 Q4 (NEAT)
Q_{CO} (s ⁻¹) ^a	7.8×10^{27}	1.33×10^{27}	3.7×10^{26}	1.45×10^{28}
$Q_{\text{H}_2\text{CO}}$ (s ⁻¹)	$\leq 3.7 \times 10^{26}$	7.6×10^{26}	4.6×10^{26}	8.1×10^{26}
$Q_{\text{H}_2\text{O}}$ (s ⁻¹)	7.6×10^{28}	6.0×10^{28}	8.8×10^{28}	2.0×10^{29}
$Q_{\text{CO}}/Q_{\text{H}_2\text{O}}$ (%) ^a	10.3	2.2	0.41	7.2
$Q_{\text{H}_2\text{CO}}/Q_{\text{H}_2\text{O}}$ (%)	≤ 0.5	1.3	0.52	0.40

^acorrected for photoelectron impact contribution.

FIGURE CAPTIONS

Fig. 1.— CO $C - X$ (0,0) band in comets McNaught-Hartley, C/2001 A2, C/2000 WM1 and C/2001 Q4. The model fit is shown together with the “cold” (dotted) and “hot” (dashed) components. P(40) indicates the position of the P-branch transitions originating from J levels near the peak of the hot, non-thermal rotational distribution seen in laboratory photodissociation experiments (van Zee et al. 1993). The corresponding R-branch lines lie below the short wavelength cut-off of the LiF2a detector. For C/2001 Q4, the gray line represents the vertical scale expanded by a factor of 10 to enhance the visibility of the non-thermal peak.

Fig. 2.— O VI pumped H_2 lines in the *FUSE* spectrum of comet C/2001 Q4. The wavelength scale is in the comet’s rest frame. The exposure time for the LiF1a channel (left panel) was 67,360 s, while the other two panels include the sum of LiF1b and LiF2a with a total exposure time of 137,530 s. The feature indicated by (*) is identified as solar Lyman- α pumped fluorescence of H_2 in the Lyman (1,1)P(5) and R(6) lines. The Lyman (6,3)P(1) line is pumped by solar Lyman- β .

Fig. 3.— Solar O VI line profile derived from an instrumentally scattered *FUSE* spectrum. The position of the Werner (1,1) Q(3) line is shown as the dashed line. The heliocentric Doppler shifts of the four comets studied are indicated as (a) C/2001 A2, (b) McNaught-Hartley, (c) C/2001 Q4, (d) C/2000 WM1.

Fig. 4.— Same as Fig. 1 for the CO $B - X$ (0,0) band. The predicted solar fluorescence brightness is shown for both the “cold” (dotted) and “hot” (dashed) components. The shape of the neighboring O I $\lambda 1152.15$ feature reflects the spatial distribution of the emitter in the *FUSE* aperture.

Fig. 5.— Cross sections for electron impact excitation (from Shirai et al. 2001). The curves

labeled (B) and (C) are for excitation of CO to produce $B - X$ (0,0) and $C - X$ (0,0) band photons, respectively, while (a) represents electron impact dissociation of CO_2 into the $a^3\Pi$ state of CO. The dashed curve represents a theoretical photoelectron energy distribution (from Körösmezey et al. 1987).

Fig. 6.— Temporal variability of the CO $C - X$ and $B - X$ bands in comet C/2001 A2. The horizontal bars indicate the individual exposures. The visual brightness deduced from the *FUSE* Fine Error Sensor is also shown.

Fig. 7.— Temporal variability of the CO $C - X$ band in comet C/2001 Q4. The origin of time is UT 2004 April 24 00:40:32. The solid line is a sinusoidal fit with a period of 17.0 h and an amplitude of 22%.

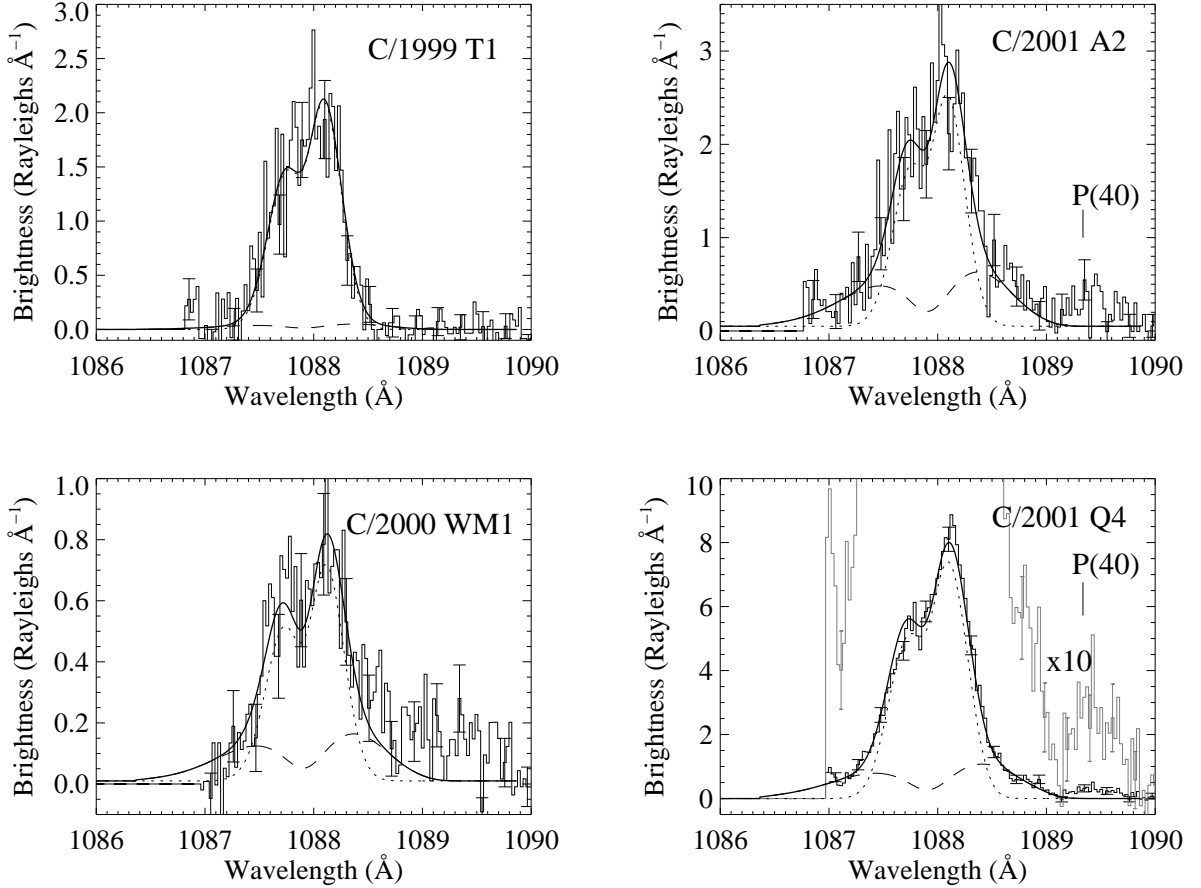


Fig. 1.— CO $C - X$ (0,0) band in comets McNaught-Hartley, C/2001 A2, C/2000 WM1 and C/2001 Q4. The model fit is shown together with the “cold” (dotted) and “hot” (dashed) components. P(40) indicates the position of the P-branch transitions originating from J levels near the peak of the hot, non-thermal rotational distribution seen in laboratory photodissociation experiments (van Zee et al. 1993). The corresponding R-branch lines lie below the short wavelength cut-off of the LiF2a detector. For C/2001 Q4, the gray line represents the vertical scale expanded by a factor of 10 to enhance the visibility of the non-thermal peak.

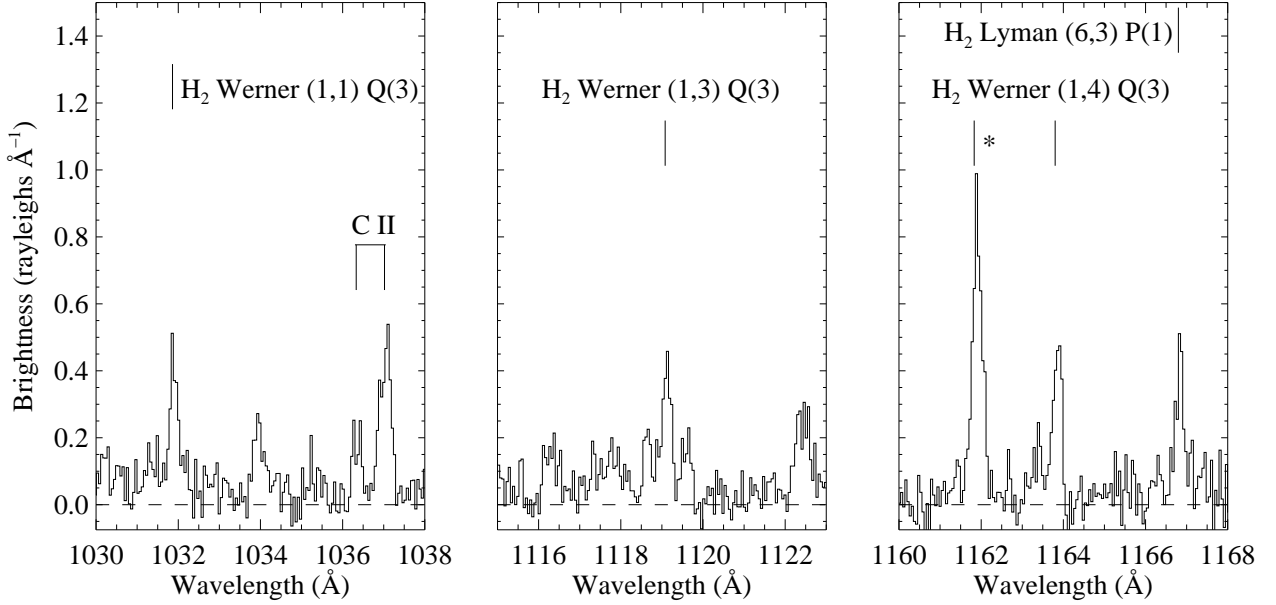


Fig. 2.— O VI pumped H₂ lines in the *FUSE* spectrum of comet C/2001 Q4. The wavelength scale is in the comet’s rest frame. The exposure time for the LiF1a channel (left panel) was 67,360 s, while the other two panels include the sum of LiF1b and LiF2a with a total exposure time of 137,530 s. The feature indicated by (*) is identified as solar Lyman- α pumped fluorescence of H₂ in the Lyman (1,1)P(5) and R(6) lines. The Lyman (6,3)P(1) line is pumped by solar Lyman- β .

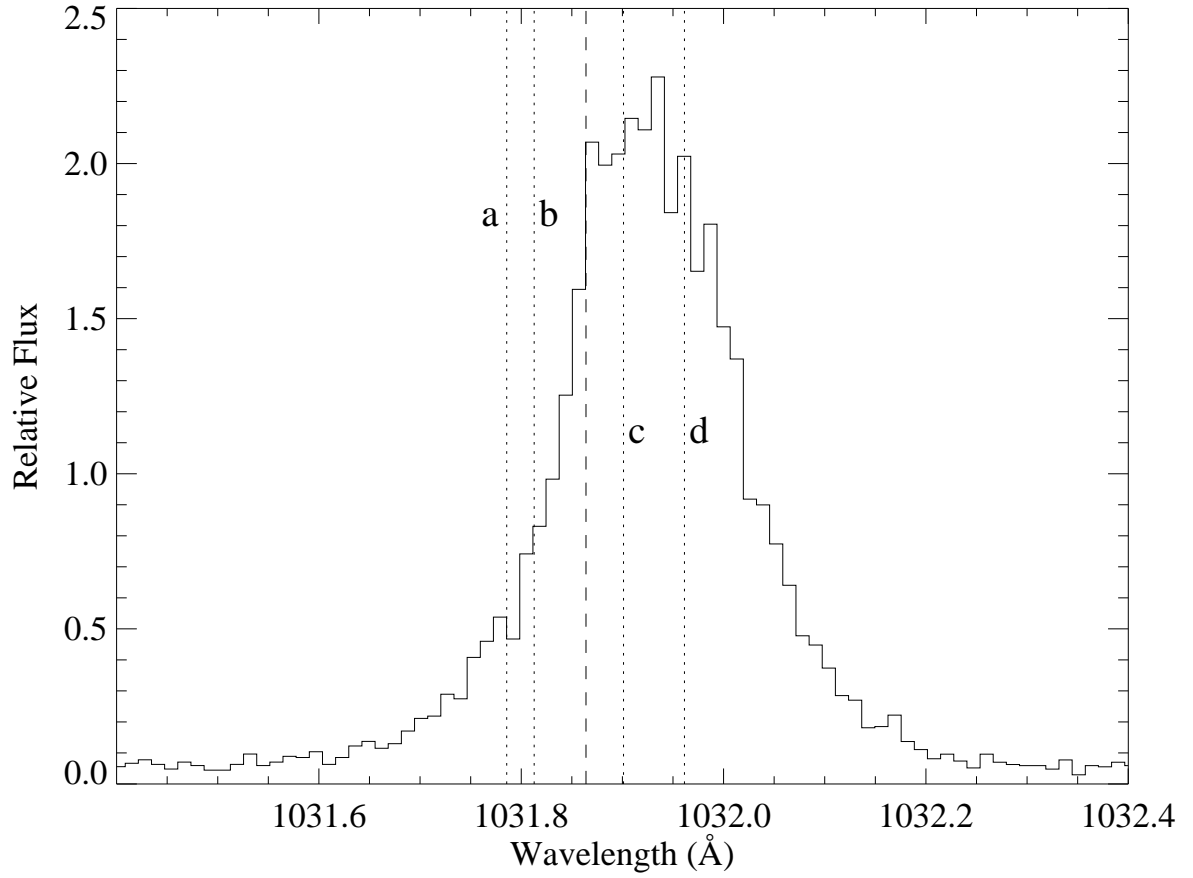


Fig. 3.— Solar O VI line profile derived from an instrumentally scattered *FUSE* spectrum. The position of the Werner (1,1) Q(3) line is shown as the dashed line. The heliocentric Doppler shifts of the four comets studied are indicated as (a) C/2001 A2, (b) McNaught-Hartley, (c) C/2001 Q4, (d) C/2000 WM1.

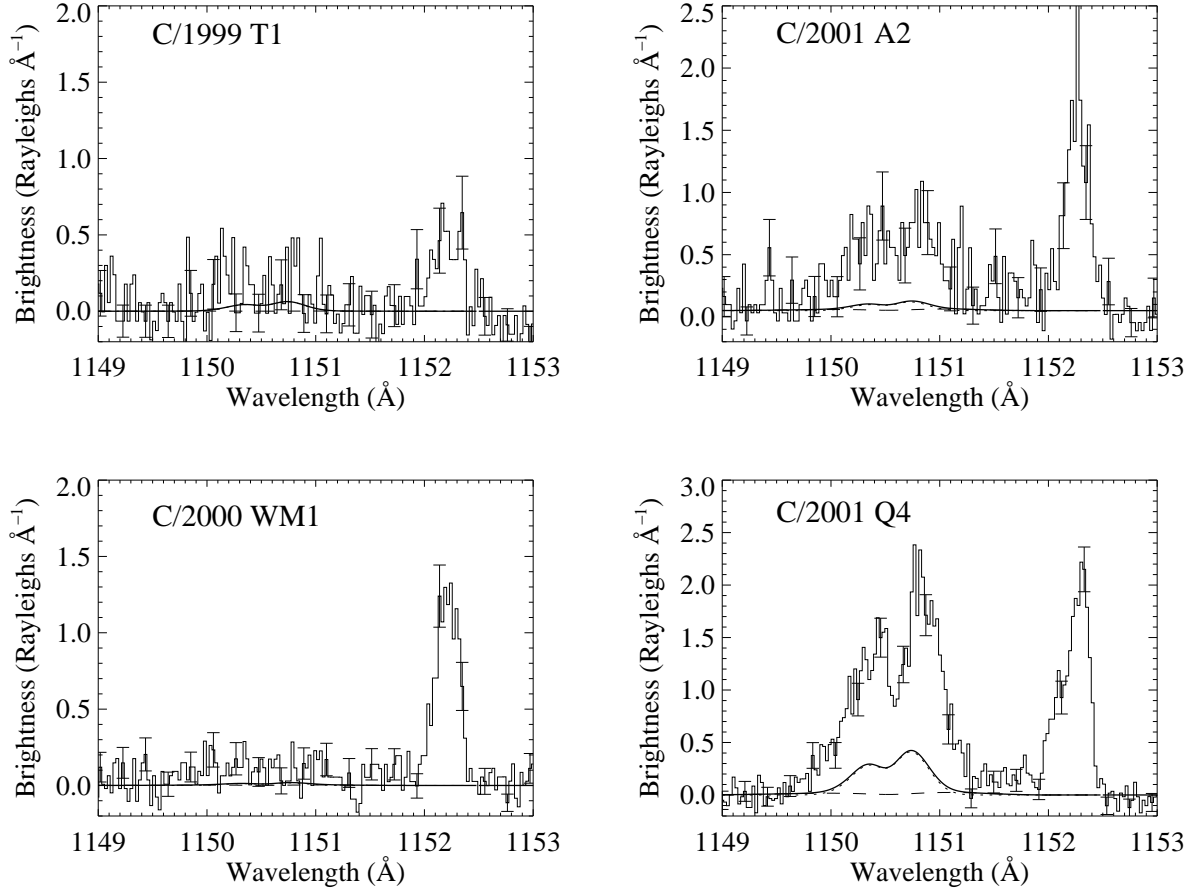


Fig. 4.— Same as Fig. 1 for the CO $B - X$ (0,0) band. The predicted solar fluorescence brightness is shown for both the “cold” (dotted) and “hot” (dashed) components. The shape of the neighboring O I $\lambda 1152.15$ feature reflects the spatial distribution of the emitter in the *FUSE* aperture.

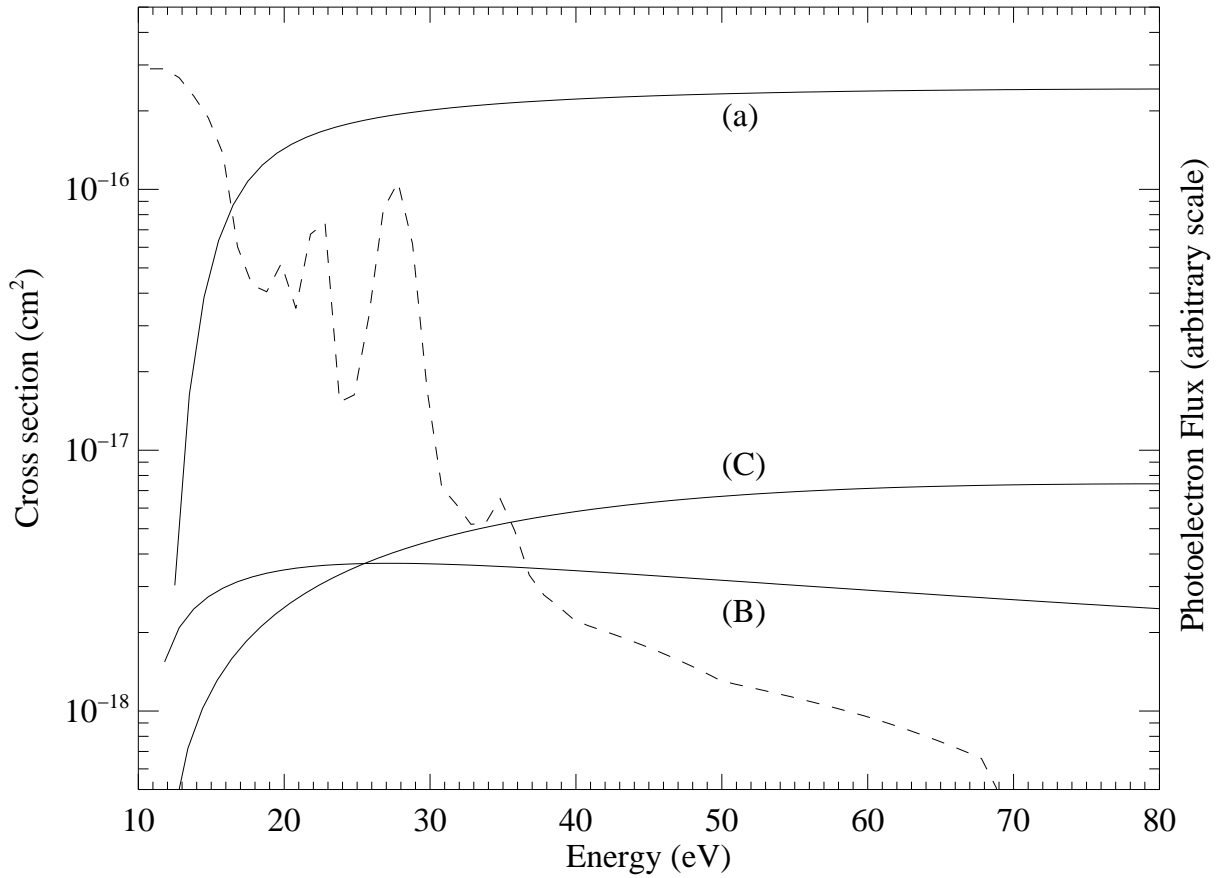


Fig. 5.— Cross sections for electron impact excitation (from Shirai et al. 2001). The curves labeled (B) and (C) are for excitation of CO to produce $B - X (0,0)$ and $C - X (0,0)$ band photons, respectively, while (a) represents electron impact dissociation of CO_2 into the $a^3\Pi$ state of CO. The dashed curve represents a theoretical photoelectron energy distribution (from Körösmezey et al. 1987).

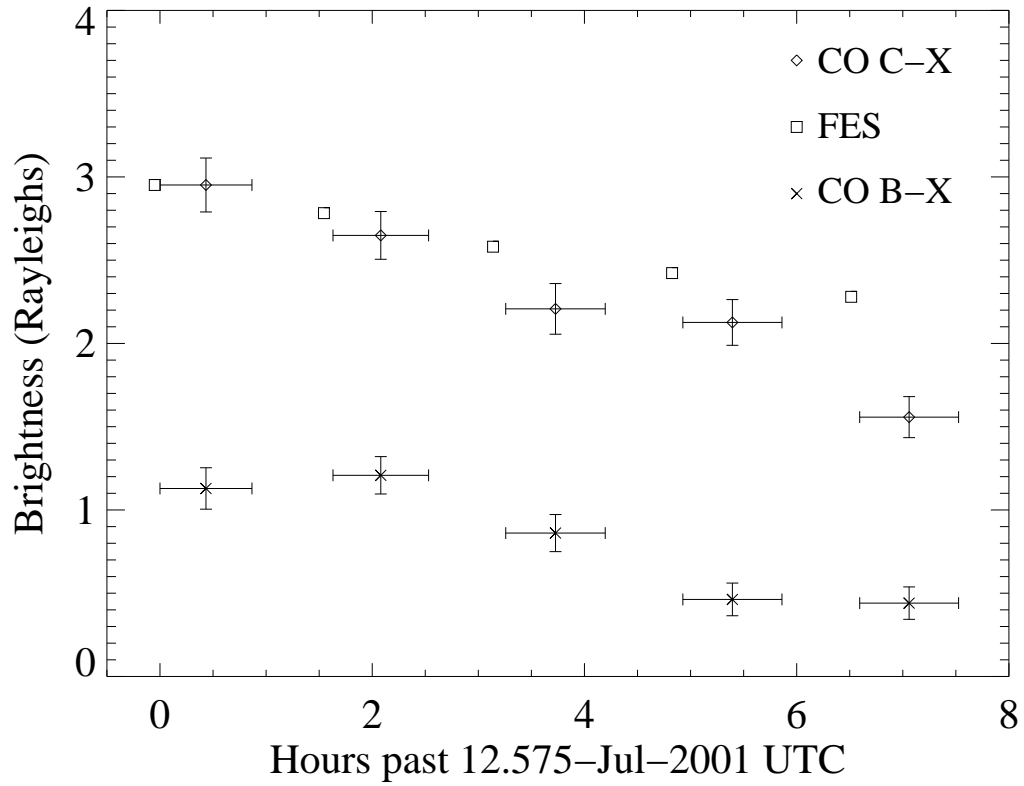


Fig. 6.— Temporal variability of the CO $C - X$ and $B - X$ bands in comet $C/2001 A2$. The horizontal bars indicate the individual exposures. The visual brightness deduced from the *FUSE* Fine Error Sensor is also shown.

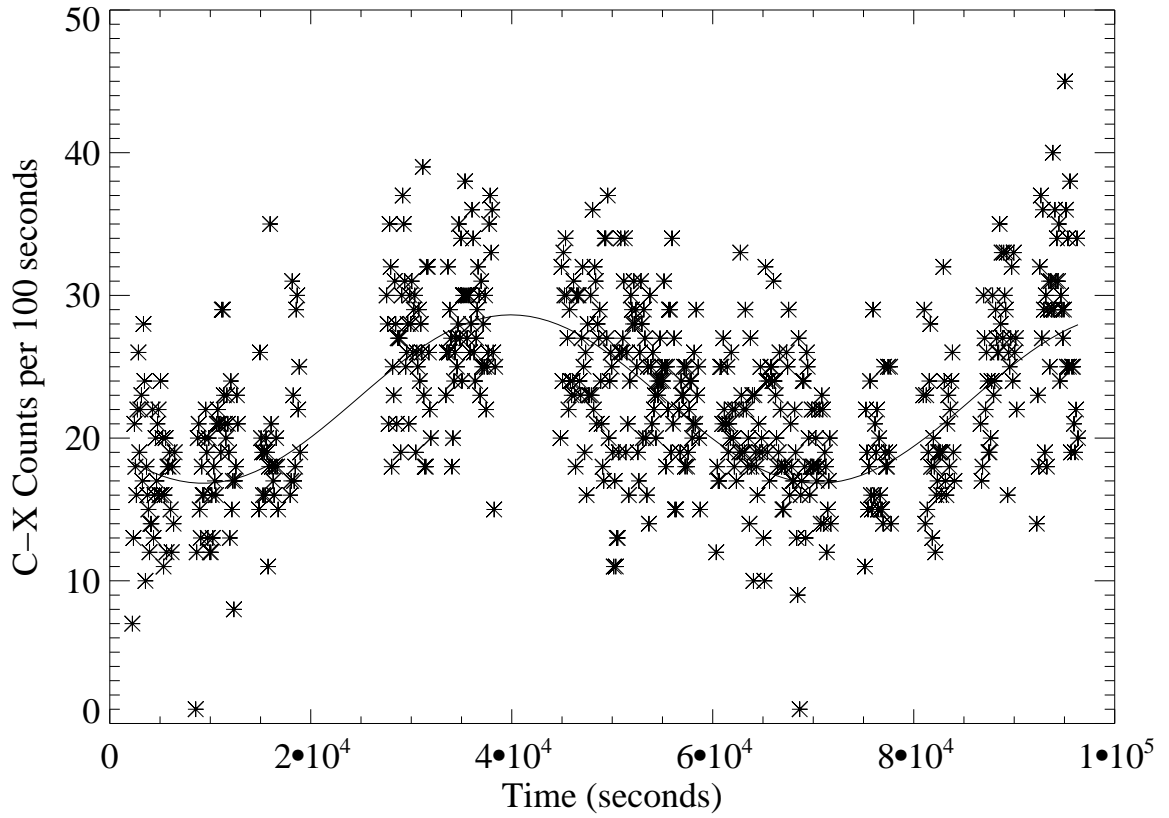


Fig. 7.— Temporal variability of the CO $C - X$ band in comet C/2001 Q4. The origin of time is UT 2004 April 24 00:40:32. The solid line is a sinusoidal fit with a period of 17.0 h and an amplitude of 22%.